Spectral measurement of the nonlinear refractive index in ZnSe using self-bending of a pulsed laser beam

Y. J. Ding, C. L. Guo, G. A. Swartzlander, Jr., J. B. Khurgin, and A. E. Kaplan

Department of Electrical and Computer Engineering, The Johns Hopkins University, Baltimore, Maryland 21218

Received April 3, 1990; accepted October 12, 1990

The nonlinear refractive-index (n_2) spectrum of ZnSe near the band gap ($\lambda_{gap} \sim 450$ nm) at 77 K was measured for the first time to our knowledge by using self-bending of a pulsed laser beam. The maximum nonlinearity, $n_2 \sim 1.9 \times 10^{-8}$ cm^2/W, measured by us is anomalously large, which cannot be explained by conventional thermally induced band-gap shrinkage.

ZnSe is one of the semiconductor materials with large nonlinear refractive index,[1–5] especially in the blue domain ($\lambda_{gap} \sim 450$ nm at 77 K). Although it is believed that the nonlinearity of ZnSe is basically due to thermally induced band-gap shrinkage[2,3] (TIBS), the nonlinear mechanisms are still not completely understood. Substantial information on the origin of the nonlinearity could be found from the measurements of the spectrum of nonlinear refractive index (Δn) in the vicinity of resonant transitions (e.g., excitonic or band-edge transitions). Recently many new Δn measurement techniques have been proposed, such as self-defocusing to determine Δn for some specific wavelengths in InSb (Ref. 6) and the Z-scan technique[7] (which measures the effective nonlinear focal length and is essentially based on external self-focusing[8]), for measuring the nonlinear refractive index n_2 of ZnSe at two specific laser wavelengths.[4] One of the natural candidates for the Δn measurements is also the so-called self-bending (SB) effect, first proposed in Ref. 9 and subsequently observed[10] in the pulse regime in NaCl crystal and recently in CS_2 (Ref. 11); the first cw measurement was done in sodium vapor.[12] In this Letter we use the SB effect for what is to our knowledge the first time to measure the spectrum of the nonlinear refractive index of ZnSe in the vicinity of the band gap.[5]

An ideal case of SB occurs when a slab beam with a triangular spatial intensity profile, $I(y)$, propagates through a Kerr-like nonlinear medium[9,13,14] to form a light-induced prism. If the nonlinear component of the refractive index is $n_2 I$, where n_2 is the coefficient of nonlinearity, the beam will be self-deflected in the far-field region by the angle θ_{NL},

$$\theta_{NL} = n_2 L I_0 / a_0, \tag{1}$$

where a_0 is the beam size, L is the thickness of the nonlinear medium, and I_0 is the laser peak intensity in the nonlinear medium. For our experiment parameters we showed using Ref. 13 that a typical value for the relative error due to the use of a right-triangular model instead of a realistic semi-Gaussian profile is less than 10%. Thus the spectral distribution of n_2, $n_2(\lambda)$, can be directly obtained by measuring θ_{NL} at different laser wavelengths. The cw measurements of SB[12] in sodium vapor showed good consistency with the theory. In our experiment we observed SB in bulk ZnSe over the range 446–460 nm, with a maximum n_2 as large as 1.9×10^{-8} cm^2/W, and used it to make direct spectral measurement of n_2 in ZnSe.

The SB method for measuring the spectrum $n_2(\lambda)$ may present certain advantages over other methods. It requires (in principle) a single shot per data point (λ) (although, owing to the lack of the detection equipment required for that, our measurements here were based on multishot averaging), whereas the Z-scan technique[4,7,8] inherently involves many shots and requires high mechanical and laser shot-to-shot stability. SB also allows one to measure n_2 directly with one laser beam, in contrast to the technique that uses two (pump and probe) laser beams,[15] and the results for n_2 are obtained indirectly (by using the Kramers–Kronig transformation). Last, the sign of n_2 can be directly determined from the SB direction.

The experimental setup is shown in Fig. 1. An 8-nsec pulsed dye laser was pumped with a frequency-tripled Nd:YAG laser. The collimated beam radius ($1/e^2$) after lenses L_3 and L_4 was $\simeq$3.5 mm, and the radial spot size in the sample plane was $a_0 \sim 100$ μm (which was calculated by using all the measured parameters of the optical system). A razor blade (RB) was inserted into the collimated beam to form a semi-Gaussian intensity profile, which was then imaged onto the ZnSe sample. After passing through the ZnSe, the beam was collimated by positive lens L_6. By measuring the displacement of the peak of the SB profile D_{NL}, the SB angle is determined to be $\theta_{NL} \simeq D_{NL}/L_6$. The samples were 500-$\mu$m-thick single-crystal ZnSe cut from the large (1 cm × 1 cm × 2 cm) ZnSe boules grown by the modified zone-melting method.[16] All the measurements were done at 77 K.

The SB intensity profile in the far-field area was obtained by scanning a pinhole across the laser beam and detecting the signal with a silicon photodiode connected to a boxcar integrator (gate width set to ~10 nsec). Typical far-field intensity profiles are shown in Fig. 2 ($\theta_{NL} \simeq 3.2$ mrad at $\lambda \sim 447.6$ nm). From the direction of SB it follows that n_2 is positive. The

0146-9592/90/241431-03$2.00/0

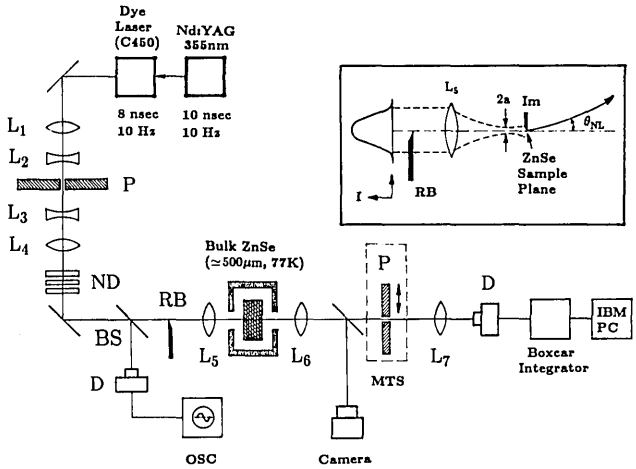

Fig. 1. Schematic diagram of the experiment. The inset shows a razor blade inserted into the beam to form a semi-Gaussian beam profile, which is then imaged onto the ZnSe sample plane. The beam is self-deflected toward the razor image because $n_2 > 0$. P's, pinholes; ND, neutral-density filter; BS, beam splitter; D's, photodiodes; OSC, oscilloscope; MTS, motorized translation stage; Im, image.

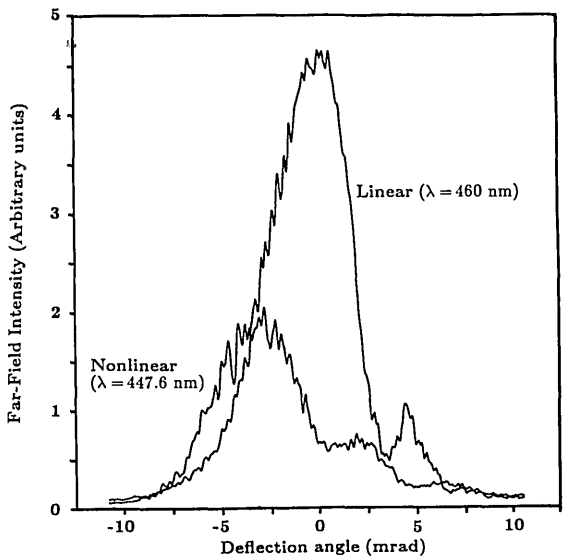

Fig. 2. Spatial intensity profiles of a laser beam in the far-field area after it passes through ZnSe plotted versus the deflection angles for linear and nonlinear cases.

secondary peaks on the profile correspond to asymmetrical diffraction rings that accompany SB, similar to the subpeaks in Ref. 12. It can be seen from Fig. 3 that as the laser wavelength is tuned away from that of the band edge, the far-field intensity profile first changes significantly but then remains essentially constant and therefore corresponds to a negligibly small nonlinearity (see the linear far-field profile in Fig. 2). Using Eq. (1), where $L \sim 500\ \mu$m, $a_0 \sim 100\ \mu$m, and $I_0 \sim 1.1 \times 10^5$ W/cm^2, we find that $n_2 \simeq 6.1 \times 10^{-9}$ cm^2/W. The relative error on n_2 after averaging over a number of measurements is ±5% (this does not include a possible systematic error).

The measured spectrum $\theta_{NL}(\lambda)$ is shown in Fig. 3 (the filled circles and solid curve). Intensity profiles in the far-field area are plotted in Fig. 3 for some specific wavelengths λ. θ_{NL} had a clear maximum at ~448 nm, where $\theta_{NL} \simeq 3.5$ mrad. The spectrum $n_2(\lambda)$ can be calculated by using the measured spectrum of θ_{NL} and Eq. (1), which should also take absorption into consideration. Our measurement showed that the absorption may become significant near the band gap (e.g., ~30% at $\lambda \sim 448$ nm; see the inset in Fig. 3 and text below). Because of that, the term LI_0 in Eq. (1) is to be replaced by $\int_0^L I(x)dx = I_0[1 - \exp(-\alpha L)]/\alpha$, where $\alpha(\lambda)$ is the absorption coefficient (see, e.g., Ref. 14). The spectrum $\alpha(\lambda)$ in ZnSe was measured[17] at $I_0 \sim 1.5 \times 10^5$ W/cm^2 (see the inset of Fig. 3). Using measured SB angles (the solid curve in Fig. 3) with the corrected Eq. (1), we calculated the spectrum $n_2(\lambda)$ plotted in Fig. 3 (the dashed curve); the shaded area in Fig. 3 corresponds to strong band-edge absorption. Our observations indicated that ZnSe materials demonstrate Kerr-like nonlinearity with no saturation up to $I_0 \sim 3.1 \times 10^5$ W/cm^2, which was verified by the fact that the SB angles were linear in the laser intensity I_0 [see Eq. (1)].

Although there are a few known mechanisms that give rise to n_2,[1-5,18] the commonly believed dominant effect near the band gap is TIBS.[2,3] If we assume the worst-case situation in which no heat transfer takes place during a single laser pulse, the maximum increase of the local temperature in the sample due to heating with the laser pulse energy in the nonlinear medium J_{laser} is

$$(\Delta T)_{max} = (\Delta T)_0 \exp(-\alpha x),$$

$$(\Delta T)_0 \simeq J_{laser}\alpha/\pi c_p a_0^2, \qquad (2)$$

where x is the distance along the axis of the beam and

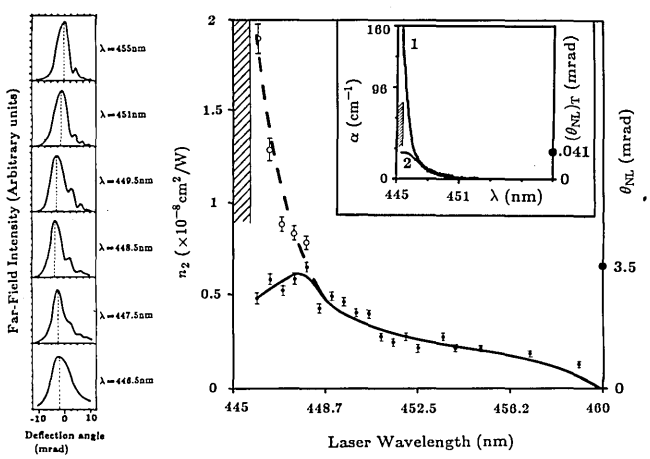

Fig. 3. Measured spectra of SB angles θ_{NL} (filled circles, experimental data; solid curve, least-square fitting) and of the nonlinear refractive index n_2 (open circles, recalculated experimental data; dashed curve, least-square fitting) versus the laser wavelength. For illustration, intensity profiles in the far-field area are plotted for some specific wavelengths at left. Inset: the measured spectra of absorption α (curve 1) and of the SB angle due to TIBS $(\theta_{NL})_T$ (curve 2) for $I_0 \sim 1.5 \times 10^5$ W/cm^2. The shaded area corresponds to strong absorption of the laser beam.

$c_p \simeq 0.34$ J/(K-cm^3) is the heat capacity of ZnSe at 80 K.[2,19] The absorption spectrum (the inset of Fig. 3) shows that the maximum absorption coefficient measured over 446–460 nm is ~74 cm^{-1} at $\lambda \sim 446$ nm. With the typical $J_{\text{laser}} \sim 2.2 \times 10^{-7}$ J, and a_0 and L as above, the absorption could increase the temperature of the sample at the boundary ($x = 0$) [Eq. (2)] by $(\Delta T)_0 \simeq 0.15$ K at $\lambda = 446$ nm. Consequently the band gap decreases by $\Delta E_g = (dE_g/dT)\Delta T$, where $dE_g/dT \simeq -8 \times 10^{-4}$ eV/K.[20] The Moss rule[21] gives the TIBS contribution to the thermal change of refractive index as $(\Delta n)_T = (-dE_g/dT)n_0\Delta T/4E_g$. By using Eq. (2) it can be translated into the total SB angle due to TIBS as

$$(\theta_{\text{NL}})_T = J_{\text{laser}} n_0(-dE_g/dT) \times \{1 - \exp[-\alpha(\lambda)L]\}/4\pi E_g c_p a_0^3, \quad (3)$$

where $n_0 \simeq 2.8$ is the linear refractive index (its linear dispersion is neglected here). The spectrum $[\theta_{\text{NL}}(\lambda)]_T$ thus calculated is plotted in the inset of Fig. 3. The peak θ_{NL} measured by us in Fig. 3 occurs at $\lambda \sim 448$ nm and is 3.5 mrad. At the same λ the SB angle calculated based on TIBS is only $(\theta_{\text{NL}})_T \sim 1.3 \times 10^{-5}$ rad, i.e., at least two orders of magnitude smaller. The errors due to some uncertainties in the calculated values of spot size, energy calibration, and other parameters cannot increase $(\theta_{\text{NL}})_T$ by more than an order of magnitude. Another (although not so strongly pronounced) difference is that whereas the TIBS spectrum plateaus near the fundamental band gap (see the inset in Fig. 3), our measured spectrum has a maximum. TIBS due to repetitive laser pulses can also be ruled out since our results were independent of repetition rate (1–10 Hz). Thus we rule out TIBS as a mechanism of the observed nonlinearity.[22] Saturation (band filling) and free-carrier effects[4,23] can also be ruled out since they both result in negative n_2.

In conclusion, the nonlinear refractive-index spectrum of ZnSe was directly measured by using the self-bending of a pulsed laser beam. It was demonstrated that this effect can provide a simple and reliable method of direct measurement of the nonlinear spectrum of semiconductor materials. Self-bending in semiconductors has the potential for such applications as the radiation protection of optical sensors and resonatorless optical bistability.[24]

We thank F. M. Davidson, C. H. Palmer, C. T. Law, X. Sun, G. Sun, and S. Li for helpful discussions and M. Shone for providing the ZnSe samples. We are indebted to both anonymous reviewers for their valuable and helpful comments. This research is supported by the U.S. Air Force Office of Scientific Research and the National Science Foundation.

References

1. D. R. Andersen, S. H. Park, S. W. Koch, and A. Jeffery, Appl. Phys. Lett. **48,** 1559 (1986); N. Peyghambarian, L. A. Kolodziejski, R. L. Gunshor, S. Datta, and A. E. Kaplan, Appl. Phys. Lett. **52,** 182 (1988).
2. G. R. Olbright, N. Peyghambarian, H. M. Gibbs, H. A. Macleod, and F. Van Milligen, Appl. Phys. Lett. **45,** 1031 (1984); I. Janossy, M. R. Taghizadeh, J. G. H. Mathew, and S. D. Smith, IEEE J. Quantum Electron. **QE-21,** 1447 (1985).
3. B. S. Wherrett, A. K. Darzi, Y. T. Chow, B. T. McGuckin, and E. W. Van Stryland, J. Opt. Soc. Am. B **7,** 215 (1990).
4. Y. Y. Wu, D. J. Hagan, E. W. Van Stryland, and M. J. Soileau, in *Digest of the OSA 1989 Annual Meeting* (Optical Society of America, Washington, D.C., 1989), p. 44.
5. Y. J. Ding, C. L. Guo, G. A. Swartzlander, Jr., J. B. Khurgin, and A. E. Kaplan, in *Digest of the OSA 1989 Annual Meeting* (Optical Society of America, Washington, D.C., 1989), p. 43.
6. D. Weaire, B. S. Wherrett, D. A. B. Miller, and S. D. Smith, Opt. Lett. **4,** 331 (1979).
7. M. Sheik-bahae, A. A. Said, and E. W. Van Stryland, Opt. Lett. **14,** 955 (1989).
8. A. E. Kaplan, Izv. Vyssh. Uchebn. Zaved. Radiofiz. **12,** 869 (1969) [Sov. Radiophys. **12,** 692 (1969)].
9. A. E. Kaplan, Pis'ma Zh. Eksp. Teor. Fiz. **9,** 58 (1969) [JETP Lett. **9,** 33 (1969)].
10. M. S. Brodin and A. M. Kamuz, Pis'ma Zh. Eksp. Teor. Fiz. **9,** 577 (1969) [JETP Lett. **9,** 351 (1969)].
11. I. Golub, Y. Beaudoin, and S. L. Chin, Opt. Lett. **13,** 488 (1988).
12. G. A. Swartzlander, Jr., H. Yin, and A. E. Kaplan, Opt. Lett. **13,** 1011 (1988); J. Opt. Soc. Am. B **6,** 1317 (1989).
13. G. A. Swartzlander, Jr., and A. E. Kaplan, J. Opt. Soc. Am. B **5,** 765 (1988).
14. V. S. Butylkin, A. E. Kaplan, Yu. G. Khronopulo, and E. I. Yakubovich, *Resonant Nonlinear Interactions of Light with Matter* (Springer-Verlag, New York, 1989), Chap. 8.
15. B. S. Wherrett and N. A. Higgins, Proc. R. Soc. London Ser. A **379,** 67 (1982).
16. S. Colak, B. J. Fitzpatrick, and R. N. Bhargava, J. Cryst. Growth **72,** 504 (1985).
17. The most recent measurements of absorption spectra done at Phillips Laboratories (Briarcliff Manor, N.Y.) by J. B. Khurgin are consistent with our measurements.
18. H. Haug and S. Schmitt-Rink, J. Opt. Soc. Am. B **2,** 1135 (1985); L. Banyai and S. W. Koch, Z. Phys. B **63,** 283 (1986).
19. P. V. Gul'tyaev and A. V. Petrov, Sov. Phys. Solid State **1,** 330 (1959).
20. B. Ray, *II–VI Compounds* (Pergamon, New York, 1969).
21. T. S. Moss, *Optical Properties of Semiconductors* (Butterworths, London, 1959), p. 48.
22. The difference between results[3] due to TIBS and our measurements may be related to the exceptionally high quality of single-crystal ZnSe material that we used compared with the polycrystalline material used in Ref. 3.
23. J. Pankove, *Optical Processes in Semiconductors* (Dover, New York, 1971), pp. 92–93; C. Kittel, *Introduction to Solid State Physics* (Wiley, New York, 1976), p. 289.
24. J. E. Bjorkholm, P. W. Smith, W. J. Tomlinson, and A. E. Kaplan, Opt. Lett. **6,** 345 (1981); A. E. Kaplan, Opt. Lett. **6,** 360 (1981).